

Update: Accurate Determinations of α_s from Realistic Lattice QCD

C. T. H. Davies,¹ I. D. Kendall,¹ G. P. Lepage,^{2,*} C. McNeile,¹ J. Shigemitsu,³ and H. Trotter⁴
(HPQCD Collaboration)

¹*Department of Physics and Astronomy, University of Glasgow, Glasgow G12 8QQ, UK*

²*Laboratory for Elementary-Particle Physics, Cornell University, Ithaca, NY 14853, USA*

³*Physics Department, The Ohio State University, Columbus, Ohio 43210, USA*

⁴*Physics Department, Simon Fraser University, Vancouver, British Columbia, Canada*

(Dated: July 8, 2008)

We use lattice QCD simulations, with MILC configurations (including vacuum polarization from u , d , and s quarks), to update our previous determinations of the QCD coupling constant. Our new analysis uses results from 5 different lattice spacings and 11 different combinations of sea-quark masses to significantly reduce our previous errors. We also correct for finite-lattice-spacing errors in the scale setting, and for nonperturbative chiral corrections to the 22 short-distance quantities from which we extract the coupling. Our final result is $\alpha_V(7.5 \text{ GeV}, n_f = 3) = 0.2121(25)$, which is equivalent to $\alpha_{\overline{\text{MS}}}(M_Z, n_f = 5) = 0.1183(7)$. We compare this with our previous result, which is about one standard deviation lower.

PACS numbers: 11.15.Ha, 12.38.Aw, 12.38.Gc

I. INTRODUCTION

An accurate value for the coupling constant α_s in quantum chromodynamics (QCD) is important both for QCD phenomenology, and as an input for possible theories beyond the Standard Model. Some of the most accurate values for the coupling constant come from numerical simulations of QCD using lattice techniques, when combined with very accurate experimental data for hadron masses. In this paper we update our previous determinations of the coupling from lattice QCD [1]. Our new analysis takes advantage of new simulation results, from the MILC collaboration, that employ smaller lattice spacings a . We also now account systematically for chiral corrections associated with the masses of sea quarks in the simulation, and for $\mathcal{O}(a^n)$ uncertainties in the values we use for the lattice spacing.

Few-percent accurate QCD simulations have only become possible in the last few years, with the development of much more efficient techniques for simulating the sea quarks; see, for example, [2] for an overview and references. The simulations we use include only light quarks (u , d and s) in the vacuum polarization; the effects of c and b quarks are incorporated using perturbation theory, which is possible because of their large masses. Our lattice QCD analysis proceeds in two steps. First the QCD parameters—the bare coupling constant and bare quark masses in the Lagrangian—must be tuned. For each value of the bare coupling, we set the lattice spacing to reproduce the correct $\Upsilon' - \Upsilon$ meson mass difference in the simulations, while we tune the u/d , s , c and b masses to give correct values for m_π^2 , $2m_K^2 - m_\pi^2$, m_{η_c} , and m_Υ , respectively; more information can be found in [2]. For efficiency we set $m_u = m_d$; this leads to negligible errors

in the analysis presented here. Once these parameters are set, there are no further physics parameters, and the simulation will accurately reproduce QCD.

Having an accurately tuned simulation of QCD, we use it to compute nonperturbative values for a variety of short-distance quantities, each of which has a perturbative expansion of the form

$$Y = \sum_{n=1}^{\infty} c_n \alpha_V^n(d/a) \quad (1)$$

where c_n and d are dimensionless a -independent constants, and $\alpha_V(d/a)$ is the (running) QCD coupling constant, with $n_f = 3$ light-quark flavors, in the V scheme [3, 4]. Given the coefficients c_n , which are computed using Feynman diagrams, we determine $\alpha_V(d/a)$ such that the perturbative formula for Y reproduces the nonperturbative value given by the simulation. Given d and a , and the c and b masses, we can then use perturbation theory to convert $\alpha_V(d/a)$ to the more conventional coupling constant $\alpha_{\overline{\text{MS}}}(M_Z, n_f = 5)$, evaluated at the mass of the Z meson.

This analysis is complicated by nonperturbative contributions to Y and by simulation uncertainties in the value of the lattice spacing a , which enters Eq. (1). It is also complicated by the fact that we only know the values of the coefficients c_n through order $n = 3$ for the quantities we examine. The main focus of this paper is to address these complications, and quantify the uncertainties in our determination of the coupling constant. In Section II we review the perturbative expansions for our short-distance quantities, all but one of which are derived from small Wilson loops [5]. The Monte Carlo simulation results for these loops are presented in Section III. We discuss finite-lattice-spacing errors and chiral corrections in Section IV. In Section V, we describe how we combine perturbation theory with simulation results using constrained (Bayesian) fitting methods. There we present

*Electronic address: g.p.lepage@cornell.edu

TABLE I: Perturbative scale and coefficients for several small Wilson loops W_{ij} and the tadpole-improved bare coupling α_{lat} . Parameters d and c_i are defined in Eq. (1).

	d	c_1	c_2/c_1	c_3/c_1
$-\log(W_{11})$	3.325	3.06840	-1.0682(2)	1.70(4)
$-\log(W_{12})$	2.998	5.55120	-0.8584(4)	1.72(4)
$-\log(W_{13})$	2.934	7.87656	-0.7435(8)	1.75(5)
$-\log(W_{14})$	2.895	10.17158	-0.6872(8)	1.70(6)
$-\log(W_{22})$	2.582	9.19970	-0.6922(10)	1.86(5)
$-\log(W_{23})$	2.481	12.34282	-0.5994(13)	2.00(6)
$-\log(W_{\text{BR}})$	3.221	4.83425	-0.8548(3)	1.80(4)
$-\log(W_{\text{CC}})$	3.047	5.29758	-0.7941(3)	1.86(4)
$\alpha_{\text{lat}}/W_{11}$	3.325	1.00000	-0.4212(2)	0.72(4)

our results and discuss in detail the various uncertainties that arise. Finally, in Section VI, we summarize our results.

II. PERTURBATION THEORY

The simplest short-distance quantities to simulate are vacuum expectation values of Wilson loop operators:

$$W_{mn} \equiv \frac{1}{3} \langle 0 | \text{Re Tr P e}^{-ig \oint_{nm} A \cdot dx} | 0 \rangle, \quad (2)$$

where P denotes path ordering, A_μ is the QCD vector potential, and the integral is over a closed $ma \times na$ rectangular path. Wilson loops should be calculable in (lattice QCD) perturbation theory when ma and na are small. We computed perturbative coefficients through order $n = 3$ for six small, rectangular loops, and also for two non-planar paths:

$$\text{BR} = \begin{array}{c} \text{---} \\ \nearrow \\ \text{---} \\ \searrow \\ \text{---} \end{array} \quad \text{CC} = \begin{array}{c} \text{---} \\ \nearrow \\ \text{---} \\ \searrow \\ \text{---} \end{array} . \quad (3)$$

The coefficients for our various loops are derived in [7]. The results are for the gluon and quark actions used to create the MILC configurations used in this study. They also assume $n_f = 3$ massless sea quarks. The quarks in our simulations are not exactly massless, but the masses are sufficiently small that the difference is negligible, $\mathcal{O}(\alpha_V^2(am)^2)$, in perturbation theory (but less so nonperturbatively, as we will discuss).

Perturbation theory is more convergent for the logarithm of a Wilson loop than it is for the loop itself. This is because the perturbative expansion of a loop is dominated by a self-energy contribution that is proportional to the length of the loop, and this contribution exponentiates for large loops. The length of the loop factors out of the expansion when you take the logarithm. This structure is evident in Table I where we tabulate the perturbative coefficients for the logarithms of our loops. The renormalization scales d/a for each quantity are determined using the procedure in [3, 4].

The perturbative coefficients in $\log(W)$, while greatly reduced by the logarithm, are still rather large. They

can be further reduced in two ways. One is to ‘‘tadpole improve’’ W_{mn} by dividing by $u_0^{2(n+m)}$ where [3]

$$u_0 \equiv (W_{11})^{1/4}. \quad (4)$$

The other is to examine Creutz ratios of the loops rather than the loops themselves [3]. Each procedure significantly reduces the known high-order coefficients: for example,

$$\log \left(\frac{W_{12}}{u_0^6} \right) = 0.949 \alpha_V (1.82/a) (1 + 0.160(2) \alpha_V - 0.54(8) \alpha_V^2 - \dots); \quad (5)$$

$$\log \left(\frac{W_{13}}{W_{22}} \right) = -1.323 \alpha_V (1.21/a) (1 - 0.39(1) \alpha_V + 0.3(2) \alpha_V^2 - \dots). \quad (6)$$

These expansions are typical of the 7 tadpole-improved loops and 6 Creutz ratios that we use in our analysis. Each has smaller α_V^3 coefficients, which improves convergence, but each also has a significantly smaller scale d/a , which slows convergence (since $\alpha_V(d/a)$ is larger).

We also include in Table I the perturbative expansion for the ‘‘tadpole-improved’’ bare coupling constant, $\alpha_{\text{lat}}/W_{11}$, where α_{lat} is the coupling constant that appears in the gluon action for a given lattice spacing. This is another short-distance quantity from which α_V can be determined.

We used Feynman diagrams to compute perturbative coefficients c_n for $n \leq 3$. Higher-order coefficients can be estimated by simultaneously fitting results from different lattice spacings to the same perturbative formula [1]. This is possible because the coupling $\alpha_V(d/a)$ changes value with different lattice spacings a :

$$q^2 \frac{d\alpha_V(q)}{dq^2} = -\beta_0 \alpha_V^2 - \beta_1 \alpha_V^3 - \beta_2 \alpha_V^4 - \beta_3 \alpha_V^5 - \dots \quad (7)$$

where the β_i are constants [6]. In this paper, we follow our earlier analysis by parameterizing the running coupling by its value at 7.5 GeV,

$$\alpha_0 \equiv \alpha_V(7.5 \text{ GeV}, n_f=3). \quad (8)$$

Given α_0 , the coupling at any other scale can be obtained by integrating Eq. (7) (which we do numerically).

Our main result will be a value for α_0 . To facilitate comparisons with other analyses, we will convert our result to the $\overline{\text{MS}}$ scheme [6], add in c and b vacuum polarization perturbatively [10], and evolve to the mass of the Z meson, again using perturbation theory [6].

III. QCD SIMULATIONS

The gluon configurations we used were created by the MILC collaboration [8]. The relevant simulation parameters are listed in Table II.

The input parameters for a QCD simulation are the bare coupling constant and bare quark masses. The coupling constant is specified through the β parameter, listed in Table II, where

$$\alpha_{\text{lat}} \equiv \frac{5}{2\pi\beta}. \quad (9)$$

The bare quark masses, $m_{0\ell}(a)$ for u/d quarks and $m_{0s}(a)$ for s quarks, used in the simulations are also listed, in units of the lattice spacing and, following MILC conventions, multiplied by u_0 (Eq. (4)). The bare masses corresponding to fixed physical masses (of, for example, pions) vary with the lattice spacing. To facilitate comparisons between lattice spacings, we use first-order perturbation theory to evolve all of our masses to a common value for the lattice spacing, which we take to be the smallest lattice spacing in our analysis:

$$m_q \equiv m_{0q}(a_{\text{min}}) \quad (10)$$

The s -quark masses here are approximately correct. The u/d masses are generally too large, but small enough to allow accurate extrapolations to the correct values.

The lattice spacing is not an input to QCD simulations. Rather it is extracted from calculations of physical quantities in the simulation. Here we use MILC's determinations of r_1/a for this purpose, where r_1 is defined in terms of the static-quark potential [8]. The values for each configuration set are listed in Table II. To obtain the lattice spacing, we need a value for r_1 . We use the value, $r_1 = 0.321(5)$ fm, determined from simulation results for the Υ' - Υ mass splitting [9]. The uncertainties quoted for r_1/a in Table II are predominantly statistical; they do not include potential errors due to the finite lattice spacing or mistuned light-quark masses, which we will discuss later.

The lattices we use here have lattice spacings that range from 0.18 fm to 0.06 fm. The spatial volumes are 2.4 fm across or larger in each case.

Our simulation results for the vacuum expectations of our 8 different Wilson loops, each for each of our 11 different configuration sets, are presented in Table III. The errors quoted are statistical errors.

IV. SYSTEMATIC ERRORS

The goal of our analysis is to determine $\alpha_0 \equiv \alpha_V(7.5 \text{ GeV})$. The only relevant systematic errors, other than from the truncation of perturbation theory, are from nonperturbative effects and from a^2 errors in our determination of the lattice spacings. Finite-volume errors are no larger than our statistical errors, as we have verified by examining configuration set 5 with $L/a = 28$ in addition to $L/a = 20$. Statistical errors are also negligible (and therefore we ignored statistical correlations between different Wilson loops when computing Creutz ratios, whose real statistical errors are 2–3 times smaller

TABLE II: QCD parameters for the 11 different sets of gluon configurations used in this paper [8]. Parameter β specifies the bare coupling constant. The inverse lattice spacing is specified in terms of the r_1 , and the bare quark masses are in units of the lattice spacing, and multiplied by u_0 . The spatial and temporal sizes, L and T , are also given. Configuration sets that were tuned to have the same lattice spacing are grouped.

Set	β	r_1/a	$au_0m_{0\ell}$	au_0m_{0s}	L/a	T/a
1	6.458	1.802(10)	0.0082	0.082	16	48
2	6.572	2.133(14)	0.0097	0.0484	16	48
3	6.586	2.129(12)	0.0194	0.0484	16	48
4	6.76	2.632(13)	0.005	0.05	24	64
5	6.76	2.610(12)	0.01	0.05	20	64
6	6.79	2.650(08)	0.02	0.05	20	64
7	7.09	3.684(12)	0.0062	0.031	28	96
8	7.11	3.711(13)	0.0124	0.031	28	96
9	7.46	5.264(13)	0.0018	0.018	64	144
10	7.47	5.277(16)	0.0036	0.018	48	144
11	7.48	5.262(22)	0.0072	0.018	48	144

than what we use here). We consider each systematic effect in term.

A. Chiral Corrections

Wilson loops, being very short-distance, are almost independent of the light-quark masses. The dependence in perturbation theory is $\mathcal{O}(\alpha_V^2(am_q)^2)$, which is negligible here given other errors. There is a larger contribution, however, from nonperturbative contributions that is important to our analysis. This contribution can be parameterized using chiral perturbation theory and the operator product expansion, which says that an arbitrary QCD operator O_{QCD} that is local at scale Λ can be expanded in terms of local operators O_n from the chiral theory:

$$O_{\text{QCD}} \equiv \sum_n c_n \frac{O_n}{\Lambda^{d_n}} \quad (11)$$

where d_n is the dimension of O_n minus the dimension of O_{QCD} . Here equivalence between the left-hand and right-hand sides means that matrix elements of the operators are equal for comparable physical states in QCD and the chiral theory.

For Wilson loops, we are interested in vacuum expectation values and singlet operators. The scale Λ for a loop of size L is $\Lambda \sim 1/L$. Consequently we expect

$$W \equiv c_0 + c_1 L \text{Tr} (m(U + U^\dagger)) + c_2 L^2 \text{Tr} (\partial_\mu U \partial^\mu U^\dagger) + \dots \quad (12)$$

TABLE III: Simulation results for the vacuum expectation values of various small Wilson loops. Results are given for each of the 11 different configuration sets.

Set	W_{11}	W_{12}	W_{13}	W_{14}	W_{22}	W_{23}	W_{BR}	W_{CC}
1	0.534101(17)	0.280720(22)	0.149263(21)	0.079710(19)	0.087438(23)	0.030150(16)	0.338982(22)	0.287376(25)
2	0.548012(51)	0.298624(68)	0.165063(67)	0.091701(63)	0.101572(73)	0.038333(54)	0.356763(68)	0.306315(78)
3	0.549470(53)	0.300310(70)	0.166530(70)	0.092797(63)	0.102640(76)	0.039007(54)	0.358570(70)	0.308140(79)
4	0.567069(16)	0.323163(21)	0.187281(24)	0.109122(27)	0.121542(19)	0.050751(15)	0.381148(25)	0.332184(27)
5	0.566961(21)	0.322987(27)	0.187084(26)	0.108927(21)	0.121341(29)	0.050579(21)	0.380988(26)	0.331996(29)
6	0.569716(21)	0.326496(27)	0.190278(26)	0.111479(21)	0.124204(29)	0.052397(21)	0.384479(26)	0.335685(29)
7	0.594843(7)	0.359761(9)	0.221624(10)	0.137271(10)	0.153433(12)	0.072261(10)	0.417002(9)	0.370239(10)
8	0.596408(12)	0.361838(19)	0.223616(17)	0.138946(16)	0.155315(18)	0.073593(16)	0.419020(16)	0.372372(17)
9	0.620813(5)	0.394837(8)	0.255897(9)	0.166723(9)	0.186116(7)	0.096208(6)	0.450947(7)	0.406300(8)
10	0.621462(3)	0.395717(4)	0.256770(5)	0.167486(5)	0.186959(5)	0.096852(5)	0.451798(4)	0.407210(5)
11	0.622115(2)	0.396607(4)	0.257650(4)	0.168257(4)	0.187809(5)	0.097491(4)	0.452654(3)	0.408123(4)

where $m = \text{diag}(m_u, m_d, m_s)$ breaks chiral symmetry, and $U \equiv \exp(i\phi/F)$ with

$$\phi = \phi^\dagger \equiv \begin{bmatrix} \pi^0/\sqrt{2} + \eta_8/\sqrt{6} & & \pi^+ & & K^+ \\ & \pi^- & & -\pi^0/\sqrt{2} + \eta_8/\sqrt{6} & K^0 \\ & & K^- & & \bar{K}^0 \\ & & & & -2\eta_8/\sqrt{6} \end{bmatrix} \quad (13)$$

and $F \approx 92$ MeV.

Taking the vacuum expectation value and a logarithm, and keeping only the leading $\mathcal{O}(a)$ terms, we get

$$\begin{aligned} \log\langle W \rangle &\approx w^{(0)} \left(1 + w_m^{(1)} a \langle \text{Tr}(m(U + U^\dagger)) \rangle \right) \\ &\approx w^{(0)} \left(1 + w_m^{(1)} a (2m_l + m_s) + \dots \right). \end{aligned} \quad (14)$$

Standard methods can be used to compute higher-order corrections, including chiral logarithms, from the expansion of $\text{Tr}(m(U + U^\dagger))$, but these are too small to be relevant to our analysis.

The leading contribution, $w^{(0)}$, is obtained from the perturbative analysis discussed in Section II, provided the loops are sufficiently small to be perturbative. We expect $w_m^{(1)}$ to be roughly independent of loop size since $w^{(0)}$ is approximately proportional to L/a (see Section II).

We can estimate the size of $w_m^{(1)}$ from a simple argument. For light-quark hadrons, hadronic quantities like meson decay constants or baryon masses depend approximately linearly on the masses of their valence quarks. The mass m_v of a valence quark makes a contribution of order $Q m_v/\Lambda$ to some hadronic quantity Q , where Λ is a momentum scale characteristic of the size of the hadron (\approx the chiral scale, for light-quark hadrons). From ratios of decay constants like f_K/f_π or of baryon masses like $m(\Lambda^0)/m(p^+)$, it is clear that m_s/Λ is of order 20%, and therefore that $\Lambda \approx 400$ MeV. Empirically contributions from individual sea-quark masses are 3–5 times smaller than those from individual valence-quark masses [11]. Consequently the relative contribution from a sea-quark mass m_q should be roughly $m_q/1.2$ GeV.

Now consider Wilson loops. The m_q dependence of $\log\langle W_{11} \rangle$, for example, should be much smaller than that for a light-quark hadron because the loop is much smaller than the hadron. The typical radius of such hadrons is around 1 fm, so we expect the relative contribution to W_{11} from a sea-quark mass of m_q to be approximately

$$\frac{a}{1 \text{ fm}} \frac{m_q}{1.2 \text{ GeV}} \approx \frac{am_q}{6}. \quad (15)$$

Therefore we expect $w_m^{(1)} = \mathcal{O}(1/6)$. This implies corrections to our $\log\langle W \rangle$ s, for example, of order 1–2% on the coarsest lattices and 0.3–0.5% on the finest lattices — which is large compared with the statistical errors in these quantities, and therefore important.

In most lattice calculations one wants the light-quark masses as close to their physical values as possible, so that lattice results reproduce what is seen in experiments. The situation for our Wilson loops is different, however. In our simulations here we are trying to isolate the perturbative part of the loop, in order to compare it with perturbation theory (not experiment), and the linear quark-mass dependence is a nonperturbative contamination that we want to remove. Consequently the precise values of the quark masses are not relevant so long as they are small enough that we can correct for them (or ignore them), which is the case here.

B. Gluon Condensate

The leading gluonic nonperturbative contribution comes from the gluonic condensate, $\langle \alpha_s G^2/\pi \rangle$. The contribution of the condensate to a Wilson loop is easily calculated to leading order in perturbation theory:

$$\delta W_{\text{cond}} = -\frac{\pi^2}{36} \left(\frac{A}{a^4} \right)^2 a^4 \langle \alpha_s G^2/\pi \rangle \quad (16)$$

where A is the loop area for planar loops. We remove this contribution from our Wilson loops before comparing them with perturbation theory. The value of the condensate is not well known, so we take $\langle \alpha_s G^2/\pi \rangle =$

$0 \pm 0.0012 \text{ GeV}^4$, which covers the range of expectations [12]. This correction is tiny except for the largest loops on the coarsest lattices. We nevertheless include it.

C. Finite- a Errors

In our analysis, the scale for the couplings comes from the lattice spacing, and the lattice spacing comes from measurements of r_1/a in the simulations. As for any physical quantity, lattice QCD measurements of r_1 have finite- a errors; and, using an analysis similar to that we outlined for Wilson loops, they should also be approximately linear in the sea-quark masses. Consequently we expect

$$r_1^{\text{lat}} = r_1(1 + r_{1a}^{(2)}(a/r_1)^2 + r_{1m}^{(1)}r_1(2\delta m_l + \delta m_s) + \dots) \quad (17)$$

where: $r_{1a}^{(2)} = \mathcal{O}(\alpha_V \approx 1/3)$, since the gluon action has no tree-level errors in $\mathcal{O}(a^2)$; and $r_{1m}^{(1)} = \mathcal{O}(1/6)$, following the discussion for Wilson loops. Here δm_q is the simulation's tuning error in the mass for sea-quark q — $\delta m_l \approx m_l$ for our simulations, while $\delta m_s \approx 0$. These corrections could affect our lattice spacings by as much as several percent, although the impact on α_0 is suppressed by a power of α_0 and so is much less. We allow for both corrections in our analysis.

V. ANALYSIS AND RESULTS

We have 22 different short-distance quantities in our analysis, each of which produces a separate value for $\alpha_0 \equiv \alpha_V(7.5 \text{ GeV})$. These consist of $\log(W)$ s for each of 8 Wilson loops, 6 independent Creutz ratios built from these loops, 7 tadpole-improved $\log(W)$ s, and the tadpole improved bare coupling $\alpha_{1\text{lat}}/W_{11}$. We have 11 values for each of these quantities, with one from each configuration set in Table II. In this section we discuss first the fitting method used for extracting α_0 , and then we review our results.

A. Constrained Fits

We analyze each short-distance quantity Y separately. We use a constrained fitting procedure, based upon Bayesian ideas [13], to fit the values $Y_i \pm \sigma_{Y_i}$ coming from each of our configuration sets (Table III) to a single formula. In this procedure we minimize an augmented χ^2 function of the form

$$\chi^2 \equiv \sum_{i=1}^{11} \frac{(Y_i - Y(a_i, (am_q)_i, \alpha_0, y_m^{(1)}, c_n, d))^2}{\sigma_{Y_i}^2} + \sum_{\xi} \delta\chi_{\xi}^2 \quad (18)$$

where i labels the configuration set, and

$$Y(a_i, (am_q)_i, \alpha_0, y_m^{(1)}, c_n, d) = \left(1 + y_m^{(1)}(2am_l + am_s)_i\right) \sum_{n=1}^{10} c_n \alpha_V^n(d/a_i). \quad (19)$$

The sea-quark mass dependence here is from Eq. (14). The lattice spacing in each case is determined from the simulation values for $(r_1/a)_i$ from each configuration set (Table II) using

$$a_i = \frac{r_1}{(r_1/a)_i} \left(1 + r_{1a}^{(2)}(a/r_1)_i^2 + r_{1m}^{(1)}(2r_1 m_l)_i\right), \quad (20)$$

which follows from Eq. (17), taking $\delta m_l \approx m_l$ and $\delta m_s \approx 0$, and $r_1 = 0.321(5) \text{ fm}$ [9]. Here $(r_1 m_q)_i \equiv (am_q)_i (r_1/a)_i$. Given the lattice spacing, the coupling $\alpha_V(d/a)$ is computed from α_0 by integrating Eq. (7) numerically.

The χ^2 function is minimized by varying fit parameters like the c_n . Every fit parameter in our procedure is constrained by an extra term or “prior” $\delta\chi_{\xi}^2$ in the χ^2 function. The expansion parameters c_n from perturbation theory, for example, are constrained by

$$\delta\chi_{c_n}^2 = \sum_{n=1}^{10} \frac{(c_n - \bar{c}_n)^2}{\sigma_{c_n}^2}, \quad (21)$$

which implies that the fit will explore values for c_n that are centered around \bar{c}_n with a range specified by σ_{c_n} : $\bar{c}_n \pm \sigma_{c_n}$. For $n \leq 3$, we set \bar{c}_n to the value obtained from our numerical evaluation of the relevant Feynman diagrams, with σ_{c_n} equal to the uncertainty in that evaluation. For $n \geq 4$, we set $\bar{c}_n = 0$ and

$$\sigma_{c_n} = 2.5 \max(|c_1|, |c_2|, |c_3|). \quad (22)$$

Thus the c_n s in the fit are constrained by the values obtained from our Feynman integrals where these are available (taking correct account of the uncertainties in those values), while the others are allowed to vary over a range that is 2.5 times larger than the largest known coefficient. The factor 2.5 was chosen using the empirical Bayes criterion, described in [13], applied to the $\log(W)$ s; applying the same criterion to the other quantities would have given smaller factors, but we take the more conservative factor of 2.5 for these as well.

We include seven c_n s beyond the ones currently known from perturbation theory to illustrate an important point. In reality there are infinitely many c_n s, but in practice the various uncertainties in our analysis mean that it is sensitive only to the first few. As we add c_n s the fit improves but only up to a point— $n = 6$ for $\log(W)$ s. As long as priors are included in χ^2 , terms can be added beyond this point but they have no effect on the result of the fit (including the error estimate) or on the quality of the fit. It is important to add enough c_n s so that further additions have no effect. We add terms through $n = 10$

to be sure we have reached this point, but, as it turns out, our analysis is not sufficiently accurate to yield new information about c_n s with $n > 6$ (beyond what is incorporated in the prior). By adding enough c_n s so that the fit results and errors cease changing, we guarantee that our final error estimates include the full uncertainty due to the fact that we have *a priori* values for only a few of the coefficients.

Other fit parameters, like α_0 , $y_m^{(1)}$, $r_{1a}^{(2)}$, and $r_{1m}^{(1)}$, must also have priors:

$$\delta\chi_0^2 = \frac{(\log(\alpha_0) - \overline{\log(\alpha_0)})^2}{\sigma_{\log(\alpha_0)}^2} + \frac{(y_m^{(1)} - \overline{y_m^{(1)}})^2}{\sigma_{y_m^{(1)}}^2} + \frac{(r_{1a}^{(2)} - \overline{r_{1a}^{(2)}})^2}{\sigma_{r_{1a}^{(2)}}^2} + \frac{(r_{1m}^{(1)} - \overline{r_{1m}^{(1)}})^2}{\sigma_{r_{1m}^{(1)}}^2} \quad (23)$$

We constrain $\log(\alpha_0)$ to be -1.6 ± 0.5 ; this prior has negligible effect on the fits because it is so broad (and the fits are so sensitive to α_0). Following the discussion in Section IV, we set

$$\begin{aligned} \overline{y_m^{(1)}} &= \overline{r_{1m}^{(1)}} = 0 \\ \sigma_{y_m^{(1)}} &= \sigma_{r_{1m}^{(1)}} = 1/6. \end{aligned} \quad (24)$$

We used the empirical Bayes criterion to check the width of these two priors and found that, in fact, this is the optimal width indicated by our simulation results. For $r_{1a}^{(2)}$, the empirical Bayes criterion suggested a width for the prior that is twice what we anticipated in Section IV C:

$$\overline{r_{1a}^{(2)}} = 0 \quad \sigma_{r_{1a}^{(2)}} = 2\alpha_V \approx 0.6. \quad (25)$$

We used this more conservative prior in our fits. Higher-order corrections are easily added but have no impact because the corrections are too small to matter, given the size of our other errors.

Our simulation result for $(r_1/a)_i$, which is used to determine the lattice spacing a_i for the i^{th} configuration set (Eq. (20)), is not exact. To include its uncertainty in our analysis we treat $(r_1/a)_i$ as a fit parameter, to be varied while minimizing χ^2 , but with a prior whose mean is the value measured in the simulation and whose width is the measured uncertainty (as in Table II). We can incorporate the uncertainty in the value of r_1 using the same trick, with r_1 as a fit parameter:

$$\delta\chi_{r_1}^2 = \frac{(r_1 - \overline{r_1})^2}{\sigma_{r_1}^2} + \sum_{i=1}^{11} \frac{((r_1/a)_i - \overline{(r_1/a)_i})^2}{\sigma_{(r_1/a)_i}^2} \quad (26)$$

where $\overline{r_1} \pm \sigma_{r_1} = 0.321 \pm 0.005 \text{ fm}$ [9].

The c and b masses are required to convert α_0 to $\alpha_{\overline{\text{MS}}}(M_Z, n_f = 5)$. We account for the uncertainties in these masses by including fit parameters, with appropriate priors, for them, together with parameters to account for unknown high-order terms in the $\overline{\text{MS}}$ β -function, and in the perturbative formulas for incorporating c and b vacuum polarization. We use c and b masses of $\overline{m}_c(\overline{m}_c) = 1.266 \pm 0.014 \text{ GeV}$ and $\overline{m}_b(\overline{m}_b) = 4.20 \pm 0.04 \text{ GeV}$ [10].

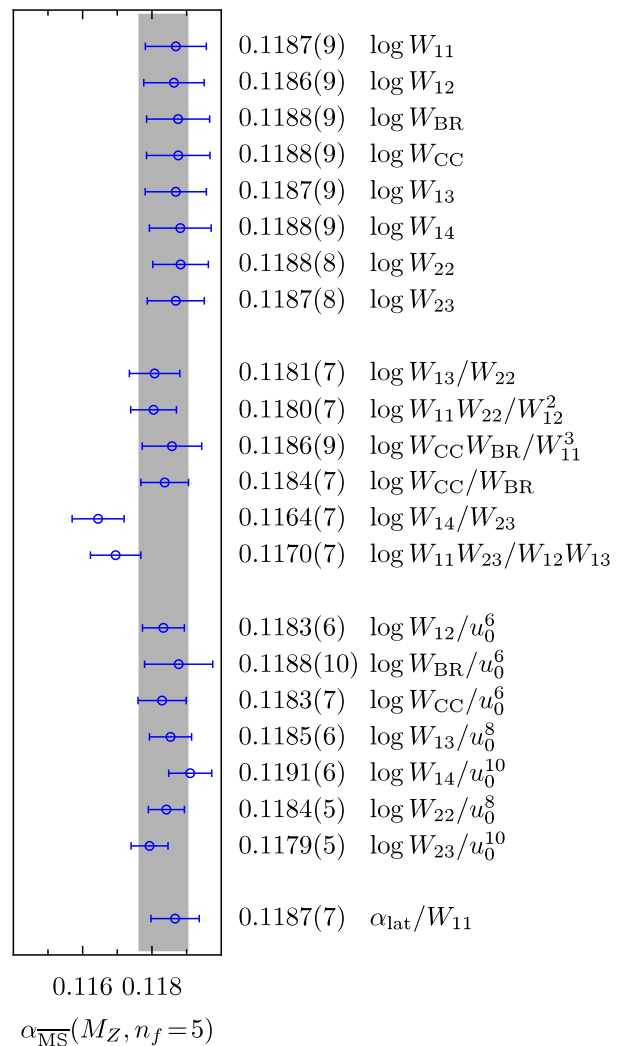


FIG. 1: Values for the 5-flavor $\alpha_{\overline{\text{MS}}}$ at the Z -meson mass from each of 22 short-distance quantities. The gray band indicates our final result, 0.1183 (7). χ^2 per data point is 0.7.

B. Results

The results from our 22 determinations of the coupling are listed and shown in Figure 1. The gray band corresponds to our final result of

$$\alpha_{\overline{\text{MS}}}(M_Z, n_f = 5) = 0.1183 (7) \quad (27)$$

which was obtained from a weighted average of all of 22 determinations [15]. Our error estimate here is that of a typical entry in the plot; combining our results does not reduce errors because most of the uncertainty in each result is systematic. The individual results in the plot are consistent with each other: $\chi^2/22 = 0.7$ for the 22 entries in Figure 1. And the fits for each quantity separately are excellent as well: $\chi^2/11 = 0.4$ to 0.7 for our fits to the 11 pieces of simulation data (one from each configuration set) for each quantity. The results in Figure 1 are derived,

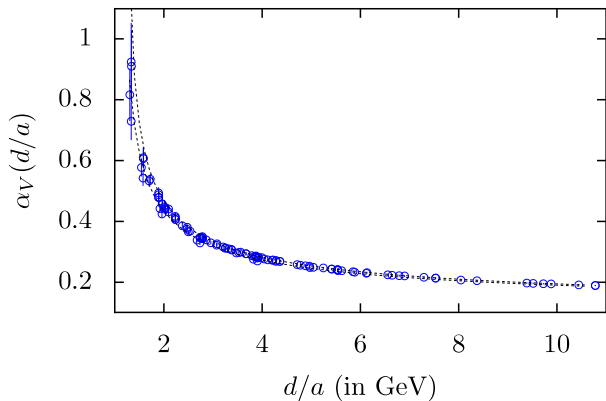


FIG. 2: Values for α_V versus d/a from each short-distance quantity at each lattice spacing. The dashed lines show predictions from QCD evolution (Eq. (7)) assuming our composite fit value (Eq. (28)).

using perturbation theory (Section II), from the fit values for α_0 , which average to

$$\alpha_0 = \alpha_V(7.5 \text{ GeV}, n_f=3) = 0.2121 \quad (28)$$

where again the error is that of a typical result for a single short-distance quantity (it is *not* reduced by one over the square root of the number of inputs).

The self-consistency of our fits is also illustrated by Figure 2, which shows the values of $\alpha_V(d/a)$ coming from every short-distance quantity for every lattice spacing in our configuration sets. The result expected from perturbative evolution (Eq. (7) with Eq. (28)), is also shown. This plot illustrates the ranges of momentum scales and α_V values that go into our analysis. The error bars give a sense of the precision with which we can determine α_V at different scales.

Although overall agreement is excellent, two of our results in Figure 1 are somewhat lower than the others. Coincidentally, perhaps, both involve W_{23} , which is the largest Wilson loop we consider. Closer examination of these two quantities did not reveal other anomalies, so it seems likely that these are simply outliers — as expected in any study of this size. Omitting these two results would increase our composite result for $\alpha_{\overline{\text{MS}}}(M_Z)$ by less than a quarter of a standard deviation, which is negligible.

It is useful to separate our error estimates into component pieces. The error estimate produced by our fitting code for a quantity like $\alpha_{\overline{\text{MS}}}$ is approximately linear in all the variances σ^2 that appear in the χ^2 function:

$$\begin{aligned} \sigma_{\alpha_{\overline{\text{MS}}}}^2 \approx & \sum_{i=1}^{11} c_{Y_i} \sigma_{Y_i}^2 + \sum_{n=1}^{10} c_{c_n} \sigma_{c_n}^2 + c_{y_m^{(1)}} \sigma_{y_m^{(1)}}^2 \\ & + c_{r_{1m}^{(1)}} \sigma_{r_{1m}^{(1)}}^2 + c_{r_{1a}^{(2)}} \sigma_{r_{1a}^{(2)}}^2 + \dots \end{aligned} \quad (29)$$

This works when errors are small, as they are here. To isolate the part of the total error that is associated with

the statistical uncertainties in the Y_i , for example, the fit is rerun but with the corresponding variances rescaled by a factor f close to one ($f = 1.01$, for example):

$$\sigma_{Y_i}^2 \rightarrow f \sigma_{Y_i}^2 \quad (30)$$

for $i = 1 \dots 11$. Then

$$\frac{\sigma_{\alpha_{\overline{\text{MS}}}}^2(f) - \sigma_{\alpha_{\overline{\text{MS}}}}^2(f=1)}{f-1} \approx \sum_{i=1}^{11} c_{Y_i} \sigma_{Y_i}^2 \quad (31)$$

The square root of this quantity is the part of the total error due to the statistical uncertainties in the Y_i . This procedure can be repeated for each prior or group of priors that contributes to the χ^2 function. The sum of the variances obtained in this way for each part of the total error should equal $\sigma_{\alpha_{\overline{\text{MS}}}}^2$; if it does not, errors may not be sufficiently small to justify the linear approximation in Eq. (29) [16].

In Table IV we present error budgets computed in this fashion for a sample of our determinations of $\alpha_{\overline{\text{MS}}}(M_Z)$. This table shows that our largest errors come from uncertainties in the perturbative coefficients with $n \geq 4$, statistical errors in the simulation values for $(r_1/a)_i$, systematic uncertainties in the physical value for r_1 , finite- a lattice errors in r_1 , and chiral effects in the W s and r_1 . Uncertainties in the parameters used to convert $\alpha_0 = \alpha_V(7.5 \text{ GeV}, n_f=3)$ into $\alpha_{\overline{\text{MS}}}(M_Z, n_f=5)$ have negligible impact. Also negligible are uncertainties due to the gluon condensate, and statistical errors in the Wilson loops.

Our errors are greatly reduced because we can bound the size of perturbative coefficients c_n for $n = 4$ and beyond. This is possible because we are fitting simulation data from five different lattice spacings simultaneously. As noted in [1], the $n = 4$ coefficients are large, particularly for $\log(W)$ s where typically our fits imply $c_4/c_1 \approx -5(2)$.

We tested the stability of our analysis procedure by omitting data and refitting. Dropping data for any one of the lattice spacings other than the smallest (configuration sets 9–11) gave results almost identical to our final result: $\alpha_{\overline{\text{MS}}}(M_Z)$ ranged between 0.1182(8) and 0.1184(8). Dropping results from the smallest lattice spacing had a bigger impact, shifting $\alpha_{\overline{\text{MS}}}(M_Z)$ to 0.1179(11) which is down by half a standard deviation and has a much larger error. A similar shift and increase in error is seen if data is discarded for all lattice spacings other than the two smallest (sets 7–11). The changes in every case that we examined were all within a standard deviation, suggesting that our procedure for estimating errors is quite robust.

Our new result is about one standard deviation above our previous result [1], and has errors that are about 40% smaller. Our new analysis differs in two important ways from our earlier work. First we include more lattice spacings, including one that is 40% smaller than the smallest we used before. (We used only configuration sets 1, 5

	$\log W_{11}$	$\log W_{22}$	$\log W_{11}W_{22}/W_{12}^2$	$\log W_{12}/u_0^6$	$\log W_{22}/u_0^8$	$\alpha_{\text{lat}}/W_{11}$
$c_1\dots c_3$	0.1%	0.1%	0.4%	0.1%	0.1%	0.1%
c_n for $n \geq 4$	0.3	0.1	0.4	0.2	0.3	0.5
$(r_1/a)_i$	0.5	0.5	0.1	0.4	0.2	0.2
r_1	0.3	0.3	0.3	0.3	0.3	0.3
am_q, r_1m_q	0.2	0.2	0.0	0.2	0.0	0.1
$(a/r_1)^2$	0.4	0.2	0.2	0.1	0.0	0.0
$V \rightarrow \overline{MS} \rightarrow M_Z$	0.1	0.1	0.1	0.0	0.0	0.1
condensate	0.1	0.1	0.2	0.2	0.0	0.1
statistical errors	0.0	0.0	0.1	0.0	0.0	0.0
Total	0.7%	0.7%	0.7%	0.6%	0.4%	0.6%

TABLE IV: Sources of uncertainties in determinations of $\alpha_{\overline{MS}}(M_Z, n_f=5)$ from various short-distance quantities. Results are given as percentages of the final result in each case.

and 7 before.) This significantly reduces the errors. Second we now use more accurate values for r_1/a . These reduce uncertainties in the ratios of lattice spacings from different configuration sets, to a third of what they were. This matters since comparing results at different lattice spacings bounds the uncalculated high-order perturbation theory coefficients in our analysis (c_n for $n \geq 4$). We are also allowing for larger finite- a errors in r_1/a on the coarsest lattices than we did previously. The changes in r_1/a , together with the smaller lattice spacing, account for most of the increase in our final result. We also now do a more systematic analysis of effects due to the sea-quark mass, fitting results with many different masses, but the effect on our final result is small: omitting the am_q corrections entirely would change our final result by less than a quarter of a standard deviation. (Our fit to $\log(W_{11})$ gives $w_m^{(1)} = -0.18(6)$, which is typical of the other fits; $r_{1m}^{(1)}$ is consistent with zero, with similar errors).

VI. CONCLUSIONS

Any high-precision determination of α_s based upon lattice QCD simulations has to address several key issues:

- *Finite-Lattice-Spacing Errors:* Errors due to the finite lattice-spacing can enter in two ways. First they affect lattice determinations of the physical quantity or quantities used to set the scale of the coupling. In our analysis we use simulation values for r_1/a , from the static-quark potential, to determine ratios of scales from different configuration sets, and simulation values for the $\Upsilon'-\Upsilon$ mass difference to set the overall scale. In each case we use data from multiple lattice spacings to bound finite- a errors, which are small because we use highly-improved discretizations in our simulations. The second source of finite- a errors, for some analyses (but not ours), is the lattice determination of the short-distance quantity that is compared with perturbation theory (to extract α_s). A short-distance

quantity that is defined in continuum QCD—for example, changes $V(r_a) - V(r_b)$ in the static-quark potential for small rs [1, 7]—will have finite- a errors that must be included in the final error analysis. The use of multiple lattice spacings is again important here. This is not an issue for us because we analyze our short-distance quantities using lattice QCD perturbation theory, which treats finite- a effects exactly (that is, to all orders in a , order-by-order in α_V). Both the simulation results and the perturbation theory for our 22 short-distance quantities are free of finite- a errors. This greatly facilitates our use of results from multiple lattice spacings to bound uncalculated higher-order terms from perturbation theory.

- *Truncation Errors from Perturbation Theory:* The coupling is determined by comparing perturbation theory with a (nonperturbative) simulation results for a short-distance quantity. Generally the perturbation theory is known through only a few low orders in α_s . The error analysis for any determination of the coupling must account for the uncalculated (but certainly present) terms from higher-order perturbation theory. We not only account for the possibility of higher-order terms (through tenth order), using our Bayesian priors, but also attempt to estimate the size of these corrections by comparing values of our short-distance quantities at five different momentum scales d/a , corresponding to our five lattice spacings. We find sizable contributions from high-order terms, particularly for $\log(W)$ s: leaving them out would shift our final result for the coupling down by two standard deviations (and lead to rather poor fits for most of our short-distance quantities). The agreement between our 22 different short-distance quantities, some with very different perturbative expansions (see Section II), is important evidence that we have analyzed truncation errors correctly.
- *Sea-Quark Vacuum Polarization:* In our previous analysis [1], we showed that the coupling is quite

sensitive to contributions from the vacuum polarization of sea quarks: $\alpha_{\overline{\text{MS}}}(M_Z)$ is 30% smaller when all quark vacuum polarization is omitted. It is therefore important to include vacuum polarization from all three light quarks. Vacuum polarization corrections from heavy quarks (c , b and t) can be computed using perturbation theory, but light quarks (u , d and s) can only be incorporated nonperturbatively. In the past we have used simulations with fewer than three light-quarks and extrapolated to $n_f = 3$ ($1/\alpha_{\overline{\text{MS}}}(M_Z)$ appears to be reasonably linear in n_f). Here (and in our previous paper), instead, contributions from all three light-quarks are included in the configurations provided us by the MILC collaboration. We also account for the small but (barely) measurable dependence upon the sea-quark masses.

- *Other Lattice and Nonperturbative Artifacts:* Usually one must worry about the finite volume of the lattice in a QCD simulation. Our Wilson loops, however, are about as ultraviolet singular as is possible on a lattice, and so are completely insensitive to the volumes of our lattices (2.5 fm across). Another issue, for continuum as well as lattice determinations of the coupling, is the possibility of nonperturbative contributions to the short-distance quantity. Our quantities are sufficiently short-distance that we do not expect appreciable nonperturbative contamination. We nevertheless allowed for nonperturbative contributions from both gluons and quarks. The expected size of nonperturbative contributions varies widely over our set of 22 different short-distance quantities and 5 different lattice spacings. The excellent agreement among all of our results is strong evidence that we understand these systematic errors.

In this (and our previous) paper, we have addressed all of these issues. We have extended our earlier analysis of the strong coupling constant from lattice QCD (and

hadronic spectroscopy) to include results from 22 different short-distance quantities computed on 11 different lattices, with 5 distinct lattice spacings and a variety of sea-quark masses. We extracted a new value for the QCD coupling by comparing these $22 \times 11 = 242$ different pieces of simulation data, covering almost an order of magnitude in momentum scales (d/a ranging from 1.3 to 10.5 GeV), with perturbation theory. Our result, $\alpha_{\overline{\text{MS}}}(M_Z, n_f = 5) = 0.1183(7)$ is in excellent agreement with our previous result and also with other non-lattice determinations (see, for example, [17, 18]).

While they are derived from the Wilson loops, our Creutz ratios and tadpole-improved loops provide coupling-constant information that is largely independent from that coming from the loops. This is because the highly ultraviolet contributions that dominate the loops largely cancel in the other quantities, making the latter far more infrared. Consequently both perturbative and nonperturbative behavior differs significantly from quantity to quantity. That all of our quantities agree on the coupling (Figure 1) is strong evidence that we understand the systematic errors involved.

The close agreement of our results with non-lattice determinations of the coupling is a compelling quantitative demonstration that the perturbative QCD of jets and the QCD of lattice simulations, which encompass both perturbative and nonperturbative phenomena, are the same theory. It is also further evidence that the simulation methods we use are valid. While early concerns about the light-quark discretization used here have been largely addressed [19, 20], it remains important to test the simulation technology of lattice QCD at increasing levels of precision. This is particularly true as lattice results become increasingly important for phenomenology.

This work was supported by NSERC (Canada), STFC (UK), the NSF and DOE (USA), and by SciDAC/US Lattice QCD Collaboration allocations at Fermilab. We also acknowledge the use of Chroma for part of our analysis [21]; and we thank Steve Gottlieb, Doug Toussaint and their collaborators in the MILC collaboration.

-
- [1] Q. Mason *et al.* [HPQCD Collaboration], Phys. Rev. Lett. **95**, 052002 (2005) [arXiv:hep-lat/0503005].
 - [2] C. T. H. Davies *et al.* [HPQCD Collaboration], Phys. Rev. Lett. **92**, 022001 (2004) [arXiv:hep-lat/0304004].
 - [3] G. P. Lepage and P. B. Mackenzie, Nucl. Phys. Proc. Suppl. **20**, 173 (1991).
 - [4] S. J. Brodsky, G. P. Lepage and P. B. Mackenzie, Phys. Rev. D **28**, 228 (1983).
 - [5] We are not yet able to update the analysis in our previous paper of the static-quark potential.
 - [6] Y. Schroder, Phys. Lett. B **447**, 321 (1999) [arXiv:hep-ph/9812205]. We take this expansion to define α_V to all orders, with no further corrections. Then β_0 through β_3 can be computed using results from T. van Ritbergen, J. A. M. Vermaseren and S. A. Larin, Phys. Lett. **B400**, 379 (1997).
 - [7] Q. Mason and H. Trottier, in preparation (2005); Q. Mason, Cornell University Ph.D. thesis (2004).
 - [8] C. Aubin *et al.*, Phys. Rev. D **70**:094505, 2004.
 - [9] A. Gray, I. Allison, C. T. H. Davies, E. Dalgic, G. P. Lepage, J. Shigemitsu and M. Wingate [HPQCD Collaboration], Phys. Rev. D **72**, 094507 (2005) [arXiv:hep-lat/0507013].
 - [10] We use the formulas from K. G. Chetyrkin, B. A. Kniehl and M. Steinhauser, Phys. Rev. Lett. **79**, 2184 (1997) with quark masses of $m_c(m_c) = 1.266(14)$ GeV from Allison *et al.* [arXiv:0805.2999] (2008) and $m_b(m_b) = 4.20(4)$ GeV [HPQCD Collaboration], in preparation (2008). For masses, see also J. H. Kuhn, M. Steinhauser and C. Sturm, Nucl. Phys. B **778**, 192 (2007) [arXiv:hep-

- ph/0702103].
- [11] This is quite obvious from lattice QCD simulations. It is perhaps because seq-quark contributions are suppressed by $1/N_c$, where $N_c = 3$ is the number of QCD colors, in a $1/N_c$ expansion of QCD.
- [12] For a recent analysis of condensate values see B. L. Ioe, *Prog. Part. Nucl. Phys.* **56**, 232 (2006) [arXiv:hep-ph/0502148].
- [13] G. P. Lepage, B. Clark, C. T. H. Davies, K. Hornbostel, P. B. Mackenzie, C. Morningstar and H. Trotter, *Nucl. Phys. Proc. Suppl.* **106**, 12 (2002) [arXiv:hep-lat/0110175].
- [14] Rather than approximating α_V by a constant, we could put in the running coupling at a scale like $2/a$. In this case, however, it makes little difference to the final fits. Our analysis is not sufficiently accurate to resolve the difference between a constant and a running coupling in the a^2 corrections.
- [15] We average our 22 different results weighted by their inverse variances, giving more weight to results with smaller variances. The variance for our composite result is the inverse of the average of the inverse variances from the separate determinations.
- [16] Occasionally the difference in Eq. (31) comes out negative. This can be caused by instabilities in the fit, in which case a different choice of f might fix the problem. It can also be the case that a term enters Eq. (29) with a negative sign. In such cases we use the absolute value of Eq. (31) for the partial variance.
- [17] A world average of 0.1176(20) is given in W.-M. Yao *et al.* (Particle Data Group), *J. Phys.* **G 33**, 1 (2006).
- [18] A world average of 0.1189(10) is given in S. Bethke, *Prog. Part. Nucl. Phys.* **58** (2007) 351 [arXiv:hep-ex/0606035].
- [19] S. R. Sharpe, *PoS LAT2006*, 022 (2006) [arXiv:hep-lat/0610094].
- [20] C. Bernard, M. Golterman, Y. Shamir and S. R. Sharpe, *Phys. Rev. D* **77**, 114504 (2008) [arXiv:0711.0696 [hep-lat]].
- [21] R. G. Edwards and B. Joo [SciDAC Collaboration and LHPC Collaboration and UKQCD Collaboration], *Nucl. Phys. Proc. Suppl.* **140**, 832 (2005) [arXiv:hep-lat/0409003].